ISSN 0965-545X, Polymer Science, Series A, 2022, Vol. 64, No. 6, pp. 573–585. © The Author(s), 2022. This article is an open access publication.
ISSN 0965-545X, Polymer Science, Series A, 2022. © The Author(s), 2022. This article is an open access publication.

REVIEW

Thermal Fractionation of Polyolefins: Brief History, New Developments and Future Perspective

X. T. Zhao[a,b] and Y. F. Men[a,b,*]

[a]*State Key Laboratory of Polymer Physics and Chemistry, Changchun Institute of Applied Chemistry, Chinese Academy of Sciences, Changchun, 130022 China*

[b]*School of Applied Chemistry and Engineering, University of Science and Technology of China, Hefei, 230026 China*

**e-mail: men@ciac.ac.cn*

Received August 11, 2022; revised September 6, 2022; accepted September 9, 2022

Abstract—For semi-crystalline polymer materials, the difference in chain structure often leads to different physical properties; therefore, in-depth analysis of the chain structure is of great significance. With the continuous development of advanced instruments, many research means have emerged to characterize the structure of molecular chains. Among them, fractionation techniques provide effectively structural information on inter- and intra-molecular comonomer distribution, branching degree, and sequence length, etc. This work briefly presents the history of developments of various classical fractionation means such as temperature-rising elution fractionation, stepwise crystallization and successive self-nucleation and annealing, while focusing on the present and future of their applications.

DOI: 10.1134/S0965545X22700419

HISTORY

In the 100 years since the "Father of polymer chemistry" Hermann Staudinger proposed the concept of "macromolecules" in 1920 [1], with the rapid development of polymer science, polymer materials of wide range of structural variations so that of very different properties have been developed. Today, polymer materials are closely related to our daily life and have long been an indispensable part. Despite the wide range of applications of polymers, exploration of their internal microstructure is still under heavy investigation.

The structure of homopolymers is relatively simple. Therefore, the characterization of its chain structure is relatively easy. But copolymers, especially the common ethylene/α-olefin copolymers (also known as linear low-density polyethylene, LLDPE), are difficult to characterize because of their complex and relatively dispersed microstructures. As is shown in Fig. 1 given by Keating et al. [2], for linear polyethylene, there is almost no interruption of comonomer units, and the crystallization ability of the chain segments is similar. Therefore, it has extremely narrow comonomer distribution (CD) and linear methylene sequence length (MSL). Once the α-olefin comonomers are inserted through the copolymerization reaction, this regular linear chain sequence will be broken, resulting in branching while broadening the CD and molecular weight distribution, forming a kind of polydisperse system. Such copolymers exhibit crystallization behavior different from those of homopolymers [3]. Macroscopically, the crystallinity of the copolymers decreases and the material properties mechanically more elastic and ductile, which is often controlled by the type and content of comonomers, copolymerization methods, catalyst systems, etc.

Qualitative and quantitative characterization of the distribution of comonomers along the molecular chain is crucial but challenging. Crystallizable chain length is the most important molecular character of polyolefins [4]. Chains of different lengths often have

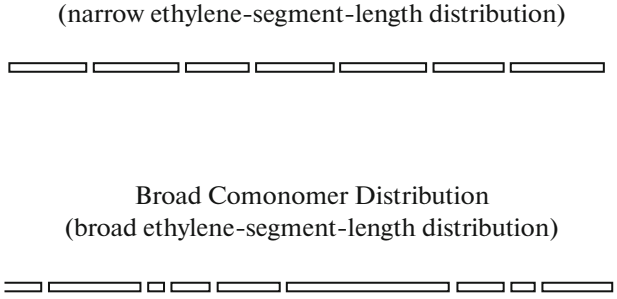

Fig. 1. Narrow and broad comonomer distributions: the blocks represent the ethylene runs and the breaks between the blocks the comonomers. Reprinted with permission of Elsevier from [3], Copyright 1994.

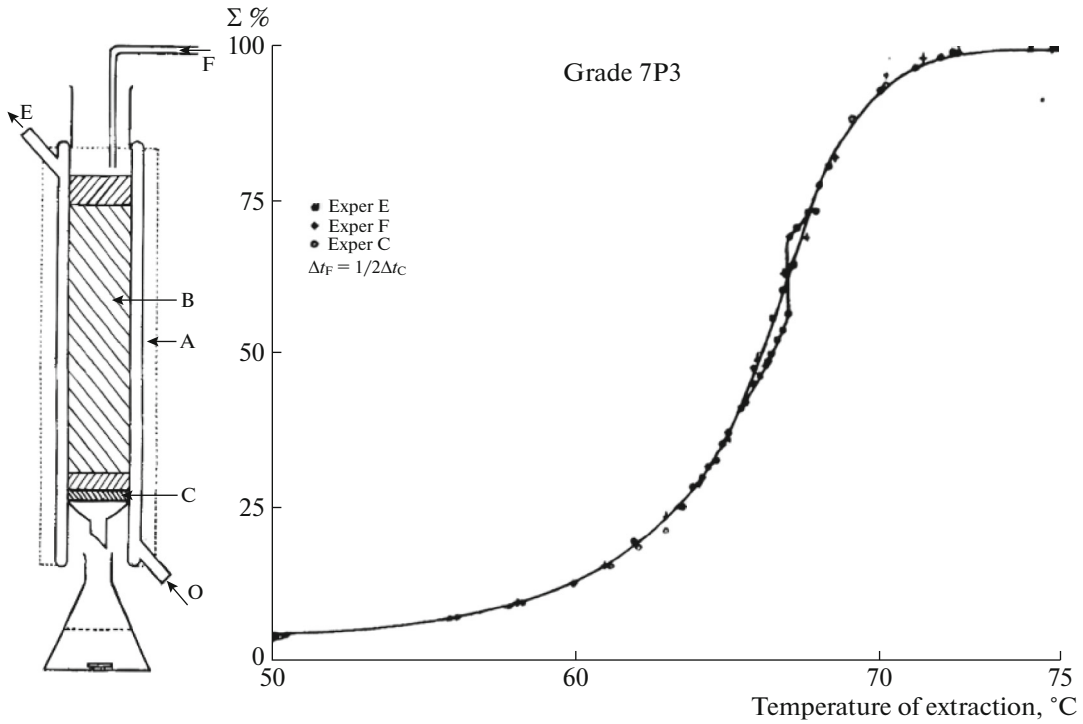

Fig. 2. Diagram of column B extraction (left) and curves of variation of solubility with temperature of graded polyacetylene (Horizontal: column temperature, Vertical: solubility), different markers represent replicate experiments (right). Replot according to [6].

different molecular chain motion ability, which further leads to significant differences in the aggregation ability of molecular chains under intermolecular or intramolecular interactions. In principle, the differences can be used to distinguish and then further separate each fraction. Since the last century, many polymer scientists have developed and applied many techniques to achieve this goal, including traditional nuclear magnetic resonance (NMR) and Fourier transform infrared spectroscopy (FTIR), and later widely used temperature rising elution fractionation (TREF), thermodynamic fractionation methods, such as step crystallization (SC) and successive self-nucleation and annealing (SSA), etc. With decades of development, these methods are used in a variety of polymers and gradually generalized.

Temperature-Rising Elution Fractionation (TREF)

The first to appear and to be used is TREF, this method often requires a large amount of solvent and is accompanied by means of volatile solvent or precipitation and centrifugation. The early prototype of this technique was proposed by Desreux et al. in 1950 [5, 6] as is given in Fig. 2. The mechanism is to select a good solvent and a series of elution temperatures, then fully dissolve the polymer on silicone carrier at each extraction temperature, and finally volatilize all the solvent in the solution eluted in each step to obtain the mass of each component, and calculate the proportion. The authors used toluene as a solvent in the fractionation of polyethylene.

In 1958, Francis et al. [7] further established a new solution fractionation technique for polyethylenes, which is suitable for both linear and highly branched polyethylene. As a modification of the previous method, the main changes included the use of a sand carrier, different ratios of solvent–nonsolvent pairs to accommodate different fractions, and a more stable temperature to ensure adequate fractionation. At the same time, the viscosity method was determined to realize quantitative calculation. Figure 3 presents the diagram of such apparatus and results for fractionation. The authors used *p*-xylene–ethylene glycol monoethyl ether (Cellosolve) mixtures as solvent–nonsolvent pairs and 15 fractions were separated.

The term "temperature rising elution technique" (TRET) first appeared in an academic paper by Shirayama et al. in 1965 [8, 9]. They modified the previous apparatus design and combined the two, using the method of Francis et al. for the first fractionation, and named it as "solvent gradient elution technique." And then, subfractions were obtained by secondary fractionation of the first fractionated fractions using the method of Desreux et al. and named as "temperature rising elution technique," as shown in Fig. 4. Furthermore, they subjected all subfractions for infrared analysis, and defined the degree of Short Chain Branches (SCB) by quantifying the absorption peaks of methyl

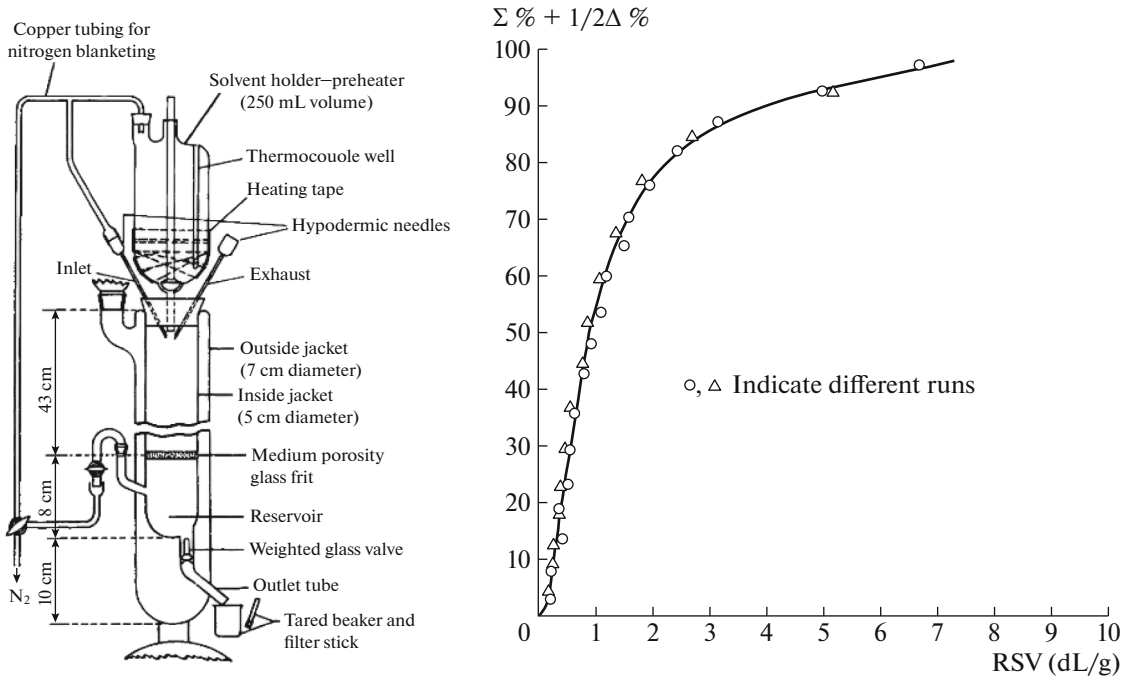

Fig. 3. Diagram of apparatus for fractionation (left) and typical integral distribution curve of linear polyethylene (Horizontal: RSV, reduced specific viscosity; Vertical: quantitative fraction), RSV is a function of molecular weight M_w (right). Reprinted with permission of Interscience Publishers, Inc., New York from [7], Copyright 1958.

groups (representing chain ends, and also the number of short branched chains), preliminarily analyzed the correlation with molecular weight and content.

With continuous revisions, the name of TREF was officially proposed by Bergstrom et al. in 1979 [10, 11]. Compared to predecessors, their modified TREF apparatus was more automatic, and the temperature control was more stable (Fig. 5 left). They synthesized a series of LDPE samples with different branching degrees by changing the temperature and pressure in the autoclave. Also combined with infrared spectroscopy, they obtained a correlation between the degree of SCB (number of CH_3 per 1000C) and the elution temperature. They also plotted each elution temperature and content distribution. And the shape of the SCB distribution was consistent with the DSC curve, proving the authenticity and reliability of the TREF experimental results.

It is generally believed that in 1982, Wild et al. [12] formally established analytical TREF as a methodology to be widely used as is given in Fig. 6. Prior to this, TREF had shown full potential in characterizing chain structure information. However, it has not been widely used due to several limitations, including excessive column size and complicated operation procedures such as filtering, drying, weighing and laminating before combining with infrared spectroscopy. They effectively reduced the column size while pairing an on-line detector for in situ measurement. The apparatus they improved is the basis for all TREF installations today. Short-branched chain distribution (SCBD), the most common concept in fractionation science, was also proposed at this time.

So far, the methodology of TREF has been well established. In the decades that followed, the method continued to be developed without more innovative changes. The current TREF includes two kinds of techniques being preparative and analytical ones, and it has also been developed from the early combination with IR to the combination of various characterization methods such as GPC, NMR, DSC, Raman spectroscopy, X-ray scattering and so on. Moreover, this method has basically been applied to all polyolefin materials and many other polymeric materials.

Nevertheless, TREF is difficult to use as a general technique for two reasons. (1) Trivial experimental process, long test cycle, large consumption of samples and solvents and high cost, etc. (2) After the process of physical separation, the polymer chain is often in a relaxed state. At this time, TREF is less sensitive to intramolecular heterogeneity than intermolecular heterogeneity.

In 1963, O'Neil and Watson of Perkin Elmer Company developed the world's first differential scanning calorimetry (DSC). This milestone invention also set the tone for the subsequent thermal fractionation means.

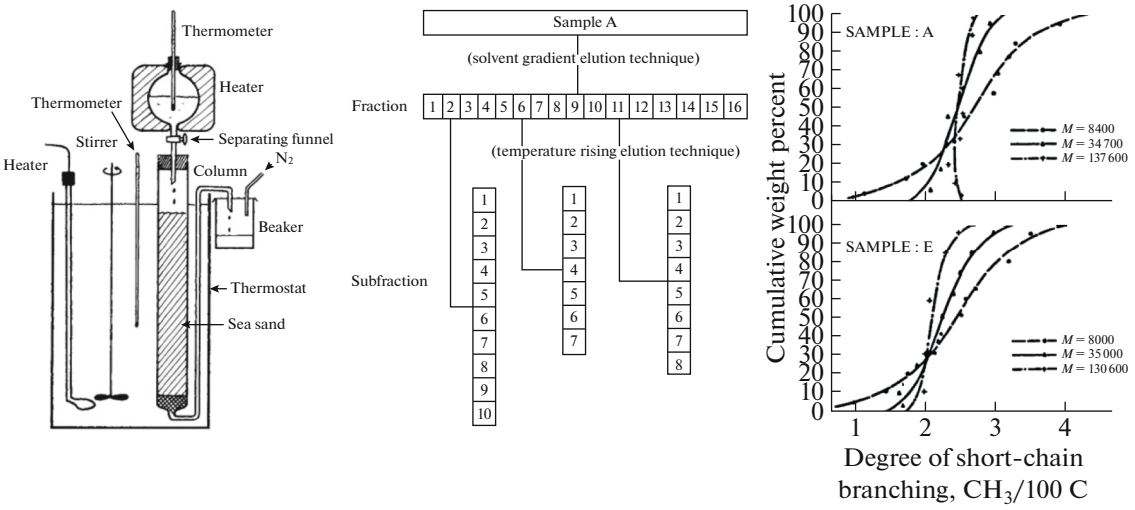

Fig. 4. Sand column elution fractionation apparatus (left), Fractionation scheme, step 1: fractionate original sample into 16 factions by SGET, step 2: fractionate primary fractions into several subfractions by TREF (middle) and Distribution of degree of SCB in fraction (Horizontal: degree of SCB, Vertical: weight percent) (right). Reprinted with permission of John Wiley and Sons, Inc. from [9], Copyright 1965.

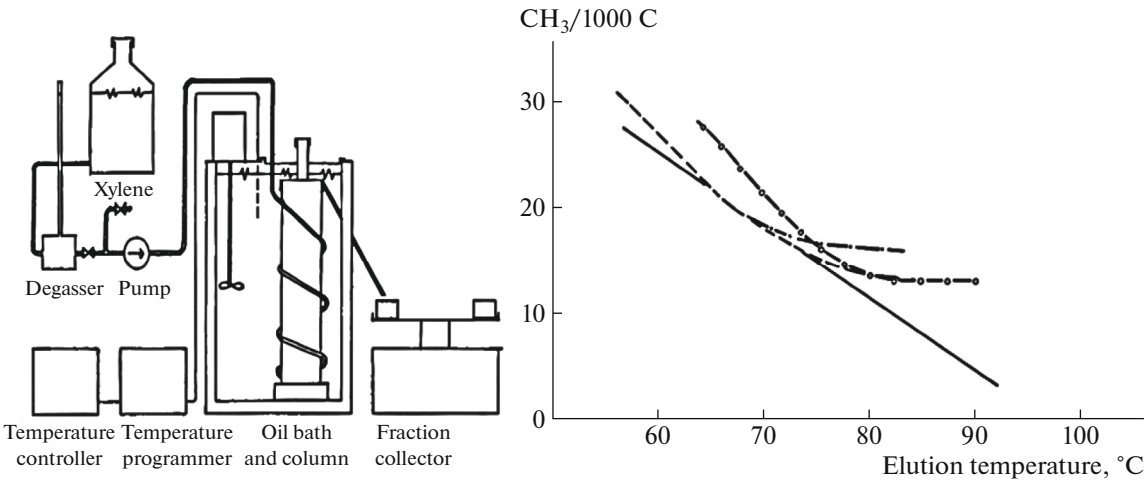

Fig. 5. Temperature rising elution fractionator (left) and methyl content of TREF fractions (Horizontal: elution temperature, Vertical: degree of SCB) (right). Reprinted with permission of John Wiley and Sons, Inc. from [11]. Copyright 1979.

Step Crystallization (SC)

SC, some scholars also termed it as stepwise isothermal segregation technique (SIS) [13] or thermal fractioned crystallization (TFC) [14] in the early days. Compared with TREF, SC needs only a conventional DSC, a small sample volume, and without solvent. Besides, this method just uses the difference in the crystallization ability of the chain segments at different temperatures to achieve a separation of different fractions. There is no physical separation in the whole process, so compared to intermolecular heterogeneity, it is equally sensitive to intramolecular heterogeneity.

The earliest thermodynamic method very similar to SC was proposed by Richardson et al. in 1963 [15]. They studied polymethylene copolymers with short branches, and for each step of crystallization to achieve thermodynamic equilibrium, the holding time of each crystallization temperature was as long as several days. Since differential scanning calorimeters were not yet available, their experiments were determined entirely by observing the relative volume changes in conventional dilatometers during melting and crystallization. But the thermal treatment they conceived is basically the same as SC.

In addition, the experimental results also gave us new insights: crystalline polymers tend to have a certain melting range during the melting process, which also means that during the crystallization process, a

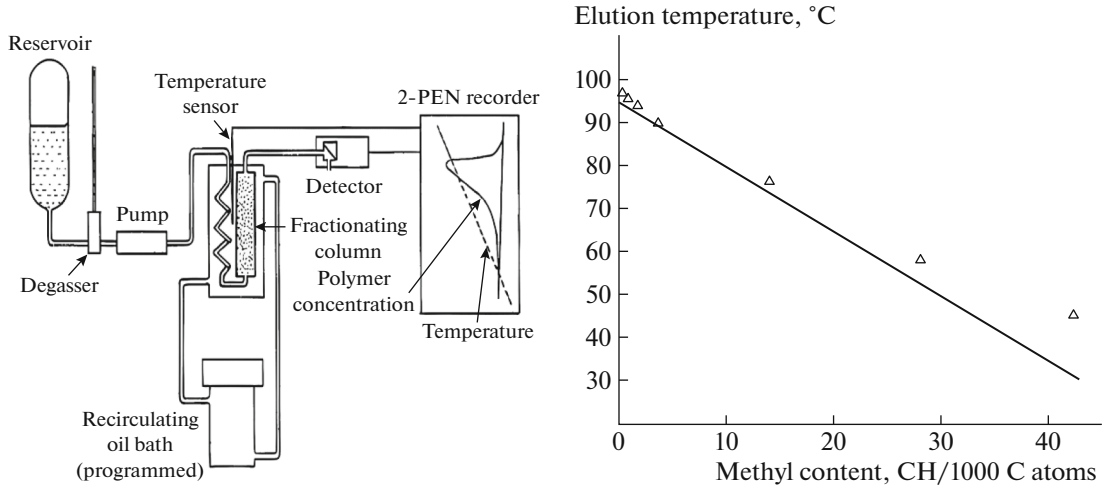

Fig. 6. Analytical temperature-rising elution fractionation system (left) and comparison of elution temperatures for linear polyethylene fractions with the calibration curve obtained using branched fractions from TREF (Horizontal: degree of SCB, Vertical: elution temperature) (right). Reprinted with permission of John Wiley and Sons, Inc. from [12]. Copyright 1982.

variety of crystals with various melting points will be formed. If one chooses a few temperatures and anneal the sample at these temperatures long enough to reach thermodynamic equilibrium at each temperature, one expects that these crystals show discrete melting points during melting.

More than ten years later, Varga et al. [16, 17] named this step-by-step annealing treatment as step crystallization (SC), and confirmed the above conjecture using DSC, which was rapidly developing at the time. At first, they named this multimodal phenomenon the "thermal memory". They designed several thermal programming schemes, as shown in Fig. 7 left.

Scheme **a** was termed as stepwise annealing. This method is very similar to successive self-nucleation annealing (SSA) technique. The difference is that the state of the Scheme **a** actually starts from the room temperature sample, while the SSA starts from the nucleation of a uniform melt at low temperature. Scheme **b** is the standard SC thermal fractionation, starting from the melt, selecting enough temperature steps during cooling, where the number of selected temperatures determines the number of peaks (n temperatures steps correspond to $n + 1$ peaks), isothermal crystallization at each annealing temperature for a certain time, and then heated to the melt state after isothermal crystallization at the last temperature, resulting in a series of discontinuous melting peaks. Scheme **c** is a combination of Schemes **a** and **b**.

Comparing the curves obtained under the three schemes, they have found that the result of SC is slightly worse than the other two. Since the self-nucleation effect at room temperature is not strong enough, they did not carry out further analysis. Nevertheless, the proposal of SC was also a milestone in the history of fractionation science, an important branch of thermal fractionation. This method was not only applied to branched polyethylene materials, but also gradually to other polyolefins. Varga et al. initially applied it to low-density polyethylene, high-pressure polyethylene and β-nucleated polypropylene (β-PP) et al. [16–18].

The principle of SC thermal fractionation is derived from TREF, but both are based on the fact that molecular chains with different degrees of branching have different crystallization abilities, and the difference is that one originates from the solution and the other originates from the melt. Compared with TREF's large solvent consumption, higher instrument requirements and complicated operation procedures, SC only needs a common differential scanning calorimeter. By contrast, there is no doubt that SC is both an efficient and simple fractionation method.

In addition, for either TREF or SC, a large amount of crystallization time is required to achieve valid fractionation. In the process of TREF, it requires long enough time to reach dissolution equilibrium. And in the process of SC fractionation, it needs long enough time to reach thermal equilibrium. Besides, it is often necessary to fully diffuse the chains. For some samples with higher molecular weights, the higher viscosity often leads to relatively poor chain diffusivity. Therefore, it is necessary to extend the holding time at each isothermal crystallization temperature to a large extent; Moreover, the extension of the annealing time tends to thicken the lamellae, forming the most stable and closer to equilibrium crystals, and then give the most accurate structural information. But at the same time, it faces the risk of sample degradation.

At the same time, another thermal fractionation technique, successive self-nucleation and annealing, which has been developed slightly later, is gradually showing its edge.

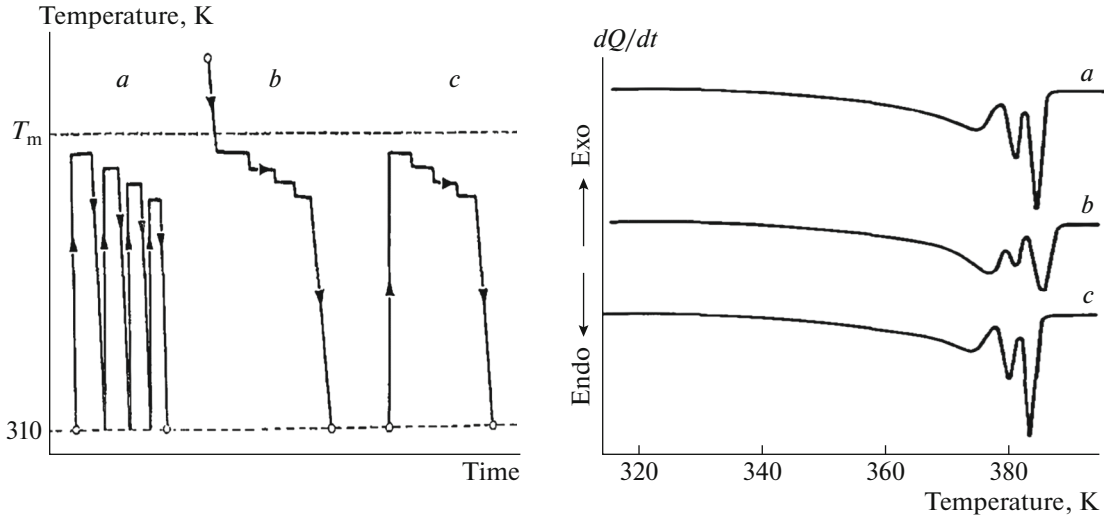

Fig. 7. The programs of stepwise heat treatments: (*a*) stepwise annealing, (*b*) stepwise isothermic crystallization, (*c*) combined method (left) and melting curves of high-pressure polyethylene samples heat treated with three methods (Horizontal: Kelvin temperature, Vertical: heat capacity) (right). Reprinted with permission of Wiley Heyden Ltd., Chichester and Akadémiai Kiadó, Budapest from [17]. Copyright 1979.

Successive Self-nucleation and Annealing (SSA)

Since the 1960s, the application of DSC has become more and more common. Many polymer scientists used this technique to explore the melting behavior of polymer materials. When studying the influence of thermal history on the melting curve, some scholars unexpectedly discovered that a discontinuous, multipeak melting curve was obtained by discontinuous annealing of the polymer.

At first, Holden believed that these discontinuous peaks were caused by different crystallization mechanisms [19]. In 1964, Gray et al. used the first power compensation DSC equipment prototype (Perkins-Elmer) to overthrow this view. They performed experiments with a continuous annealing-room temperature-annealing thermal program to process ethylene/butene copolymer (LLDPE) and linear/branched polyethylene blend, and obtained multipeak melting curves. Similar to the step annealing proposed by Varga in 1979 mentioned above, this is the earliest proposed thermal program that is very close to SSA, it can also be considered as the earliest prototype of SSA. The melting curves shown in Fig. 8 were obtained following the experimental procedures below. Fig. 8a: the sample was held at 180°C for several minutes to erase thermal history and cooled down to ambient temperature at a rate of 6 K/min followed by a heating scan to 160°C at a rate of 18 K/min. Figs. 8b–8d: the sample was cooled down from 180°C at a rate of 18 K/min to 104°C, where the onset of crystallization appeared. It was immediately heated up at 18 K/min to 120°C and annealed at this temperature for 1 min followed by a rapid cooling down to room temperature and kept for 3 min. The above procedure was repeated but the maximum temperature of heating was set to below 120°C according to a preset interval. Such procedures continued keeping the interval the same until the maximum heating temperature reached ambient temperature. Finally, the thus proceeded samples were heated up to record the fusion curves. Thus, Figs. 8b–8d present results of intervals of 10, 5, and 2 K.

The difference is still that room temperature cannot provide a strong enough self-nucleation effect for polyethylene systems. At the same time, they also adjusted one important parameter “the temperature interval”. A melting curve with higher resolution and more peaks is obtained (shown in Fig. 8). At that time, they concluded that the reason for this phenomenon may be that the effective non-linear cooling rate caused by the exotherm during the crystallization of crystals of different sizes led to transient annealing of the polymer, which caused the discontinuity of the melting peak [20].

In 1986, Varga et al. [18] used continuous annealing methods to study the β/α and β/β recrystallization behavior of β-PP. Their original purpose was mainly to study a special “melt memory effect”, i.e., β-PP often gives one melting peak after isothermal crystallization but if the sample was cooled down to room temperature after isothermal crystallization an α/β phase transition occurs, and the subsequent melting process shows the melting peaks of both the β and α forms of polypropylene.

Several thermal programs (shown in Fig. 9 left) they designed are very similar to the single cycle steps of SSA. Not only that, they selected several step annealing temperatures and performed several cycles to obtain a multimodal melting curve (Fig. 9, right). At that time, their main concern was the memory effect

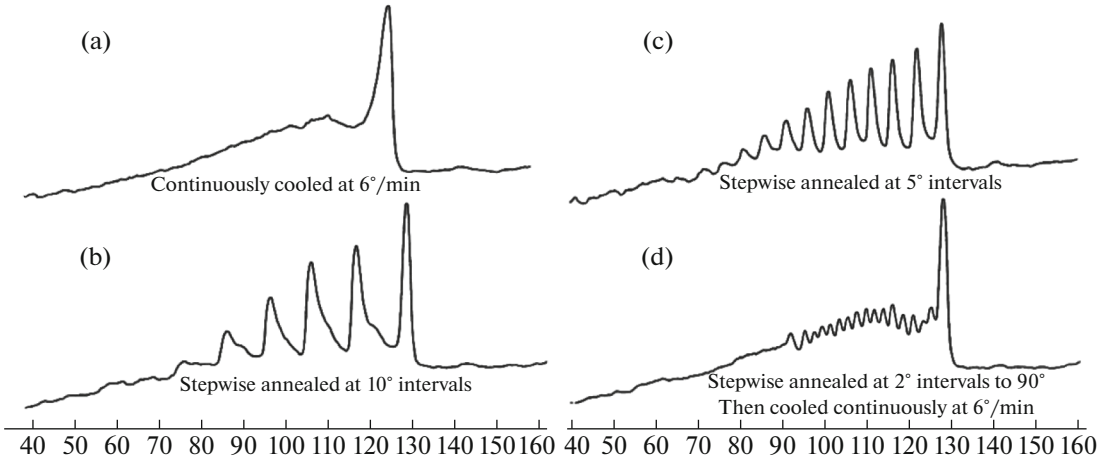

Fig. 8. Fusion curves of polyethylene blend. Same sample—different thermal histories (different temperature intervals: (b) 10, (c) 5, (d) 2 K). Scanning rate: 18 K/min. (Horizontal: degree Celsius, Vertical: heat capacity), endo up. See comments in the text. Reprinted with permission of John Wiley and Sons, Inc. from [20], Copyright 1964.

brought by the nuclei of different crystalline forms and the concept of thermal fractionation was still very vague, so they did not carry out a deeper interpretation. But the idea and thermal program was very close to SSA.

In 1993, Fillon et al. [21–23] applied DSC thermal program to the controversial self-nucleation (SN) theory (also named "melting memory effect"), which is an important part of the later SSA thermal program.

SN was first proposed by Blundell et al. in 1966 [24]. As the name suggests, it produced its own crystal nucleus in a homogeneous state, and then regulated the crystallization behavior of the entire system. Macroscopically, the crystallization rate was accelerated, or a certain crystalline form was more preferred to be generated. Initially they aimed to prepare single crystals from solution.

However, Fillon et al. were the first to propose the application of DSC measurements to the concept of self-nucleation, while using optical means to provide evidence that is visible in the macroscopic view. The thermal program designed by Fillon et al. is shown in Fig. 10 left [21]. The system studied was a sample of polypropylene.

Starting from a homogeneous melt after eliminating thermal history, quenching to a low temperature outside the crystallization temperature range to construct a repeatable "standard". Heating to different selected T_S in the melting range facilitates the preparation of self-nucleation (self-seeds) with different sizes. Secondary quenching and melting were used to study the effect of self-nucleation with different sizes on the crystallization behavior of the subsequently grown crystals. The results showed that the lower the selected T_S, the higher the secondary crystallization temperature. This means that an increasing number of self-seeds (more unmolten crystals) can effectively speed up the subsequent crystallization process.

The successful application of self-nucleation in differential scanning calorimetry gives us new inspiration, since fractionation methods such as TREF and SC require a lot of time, can this "self-nucleation" comparable to the nucleating agents be effective in the fractionation process?

Based on a series of previous work and some innovative developments, Müller et al. systematically proposed a novel thermal fractionation technique for the first time in 1997 and applied it to polyolefins, which is a very important milestone in the history of thermal fractionation. As the most commonly used thermal fractionation technique today [25], SSA can be understood as a superposition of multiple self-nucleation/annealing. Because the difference in internal chain structure leads to the formation of crystals of different sizes at different annealing temperatures, each melting peak represents a crystal with a different mean lamellar thickness, and the fraction with the highest melting point represents the thickest lamellae or longest uninterrupted linear chain segments, the small crystalline blocks or chain segments that failed to grow in this series of processes can often be used as the self-seeds for the annealing of the next fraction. The higher melting points of the fractions mean fewer SCB and longer methylene sequence length (MSL), and the narrower fraction distribution also represents a narrower distribution of chemical composition content (CCD, distribution of comonomer or number of branches).

This technique can be understood but cannot be regarded as a simple superposition, and the result of fractionation is regulated by many parameters. Figure 11 shows the standard SSA thermal program (left) designed by Müller. After eliminating the ther-

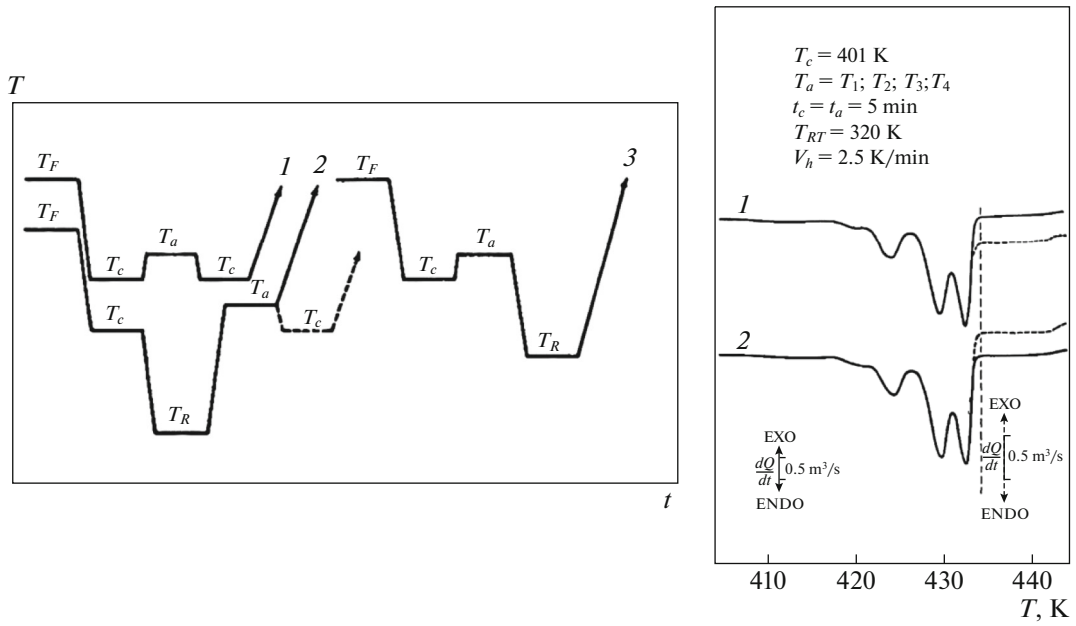

Fig. 9. Scheme of annealing temperature programs (left) and melting curves (Horizontal: Kelvin temperature, Vertical: heat capacity) (right). Reprinted with permission of Hüthig and Wepf Verlag. From [18], Copyright 1986.

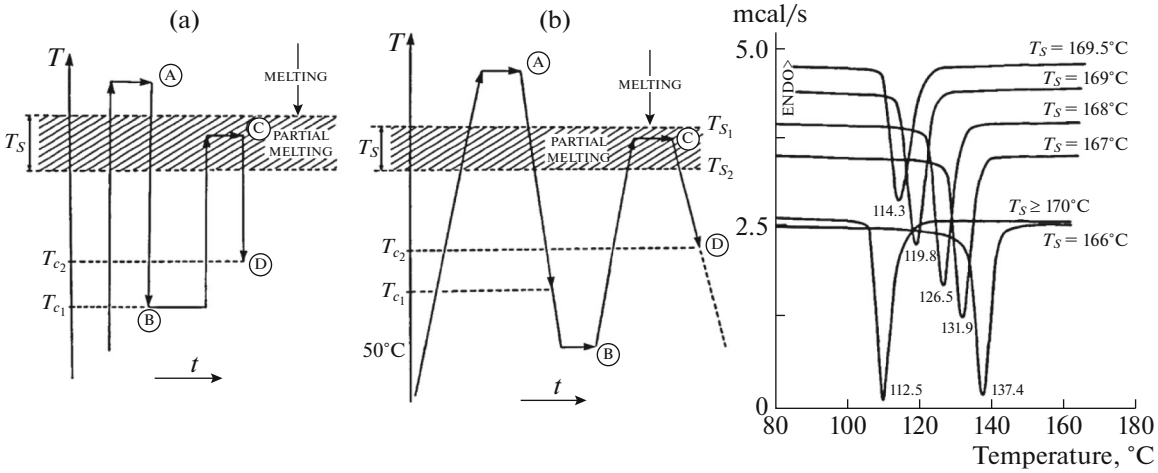

Fig. 10. The self-nucleation procedure as applied (left) and crystallization exotherms of i-PP after different degree of melting at various T_S (Horizontal: degree Celsius, Vertical: heat flow) (right). Reprinted with permission of John Wiley and Sons, Inc. from [21, 22], Copyright 1993.

mal history, dropping below the crystallization temperature range constructs a "standard". The most important parameter is the first selected T_S, and the selected range is often the best self-nucleation region, that is, Domain *II* (defined by Fillon et al.: Domain *III*: crystals exist due to incomplete melting, Domain *II*: remaining crystal fragments or entanglements in the upperpart of melting range, Domain *I*: self-nucleation effect disappears due to complete melting). The purpose is to provide enough self-seeds for following successive steps.

As for the selection of other parameters, according to the difference of the samples, the appropriate temperature interval within the melting range and appropriate annealing time can be selected.

Müller et al. also compared the results of SSA and SC fractionating the same LLDPE sample (Fig. 11 right). one can observe that SSA achieves much better fractionation in less time, not only that, the resolution is higher, and the bimodal distribution of the sample is also resolved.

In summary, compared with TREF, SSA has the same advantages as SC; compared with SC, SSA has

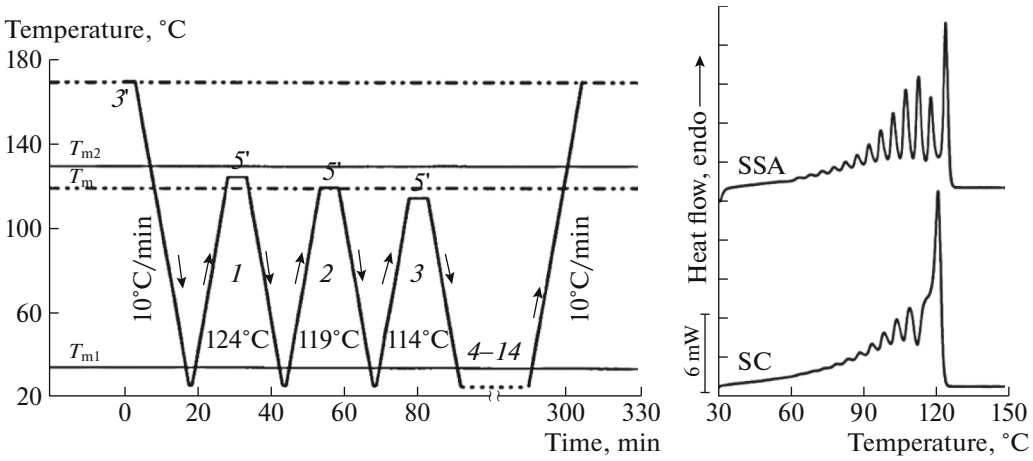

Fig. 11. Schematic representation of successive self-nucleation/annealing (SSA) thermal treatment (e.g., as applied to LLDPE) (left) and comparison of SC and SSA fractionation curves (Horizontal: degree Celsius, Vertical: heat flow) (right). Reprinted with permission of Springer-Verlag from [24], Copyright 1997.

higher resolution and higher efficiency. Among the three, SSA is the most widely used now, and has developed into an extremely powerful means to characterize the structure and distribution of molecular chains, especially for highly branched polyolefin systems. Müller, the inventor of SSA, reviewed a series of applications and improvements of the technique in 2005 [26] and 2015 [27] respectively.

QUANTITATIVE ANALYSIS

For a series of discontinuous thermal fractionation curves, it is often necessary to perform data processing by fitting software, and then quantitatively obtain molecular chain structure information.

Changes in polymerization methods, catalytic systems, etc., often result in polymers with very different chain structures. In 1989 Dow Chemical Company synthesized a metallocene catalyst called "constrained-geometry catalyst, CGC." The chain transfer of this type of catalyst will produce macromonomers with double bonds at the end of the chain, and the participation of such macromonomers in the polymerization reaction will produce long-chain branched polymers, and the degree of branching is not uniform [28]. We now express this degree of branching by SCB, defined as the number of CH_3 per 1000 carbons.

Adisson et al. [29] proposed Eqs. (1)–(6) to calculate the number of SCB of several kinds of ethylene/α-olefin copolymers using the melting point of the SSA thermal fractionation curves.

For ethylene/1-butene copolymers:

$$T_m = -1.55\mathrm{SCB} + 134 \quad (1)$$

$$X_c = -0.0132\mathrm{SCB} + 0.82 \quad (2)$$

For ethylene/1-hexene copolymers:

$$T_m = -1.69\mathrm{SCB} + 133 \quad (3)$$

$$X_c = -0.0134\mathrm{SCB} + 0.77 \quad (4)$$

For ethylene/1-octene copolymers:

$$T_m = -2.18\mathrm{SCB} + 134 \quad (5)$$

$$X_c = -0.0251\mathrm{SCB} + 0.86 \quad (6)$$

The crystallizable components in ethylene/α-olefin copolymers are often uninterrupted methylene sequences. Zhang et al. [30] further extended the Eq. (7) proposed by Keating et al. [31] to quantitatively correlate the melting point of the thermal fractionation curves with the MSL (Eq. (8)). Chen et al. also constructed the correlation between SCB and MSL by Eq. (9), so as to facilitate the mutual conversion calculation between the two [32].

$$-\ln(\mathrm{CH_2}) = -0.31767 + \frac{131.61}{T(\mathrm{K})} \quad (7)$$

$$MSL = \frac{2(\mathrm{CH_2})}{1-(\mathrm{CH_2})} \quad (8)$$

$$MSL = (998 - SCB)/(SCB + 1) \quad (9)$$

In addition, we can use the most classical Gibbs-Thomson Eq. (10) to quantitatively calculate the crystalline structure information such as lamellar thickness.

$$T_m = T_m^0(1 - 2\gamma\sigma_e/\Delta H_u l) \quad (10)$$

Keating et al. defined number average lamellar thickness l_n, weight average lamellar thickness l_w and lamellar thickness distribution I based on the concepts of number average molecular weight M_n, weight average molecular weight M_w and molecular weight distribution D [31]. They defined the calculation Eqs. (11)–

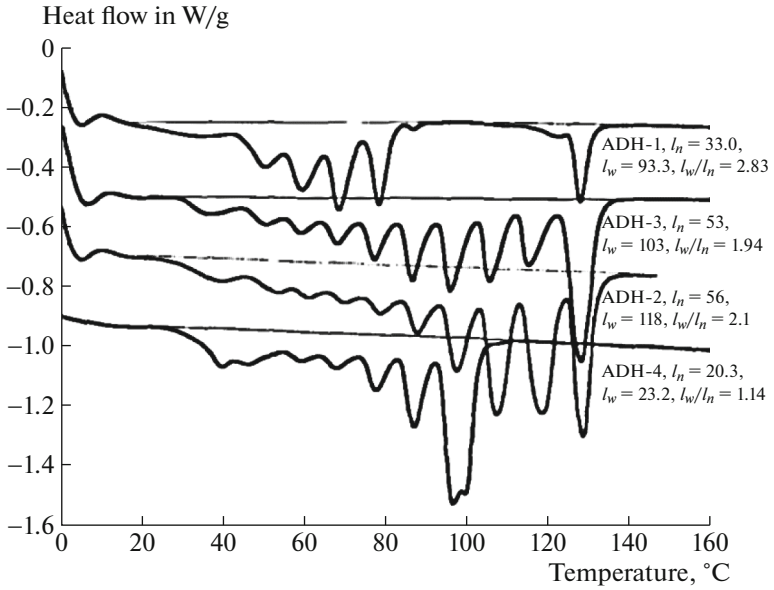

Fig. 12. Thermal fractionated adhesives (Horizontal: degree Celsius, Vertical: heat flow), identification are the quantitative calculation results. Reprinted with permission of Elsevier B.V. from [31], Copyright 1996.

(13) for the lamellar structure information through the thermal fractionation curves shown in Fig. 12.

$$l_n = (n_1 l_1 + n_2 l_2 + \cdots n_i l_i)/(n_1 + n_2 + \cdots n_i) = \sum f_i l_i \quad (11)$$

$$l_w = (n_1 l_1^2 + n_2 l_2^2 + \cdots n_i l_i^2)/(n_1 l_1 + n_2 l_2 + \cdots n_i l_i) = \sum f_i l_i^2 / \sum f_i l_i \quad (12)$$

$$I = l_w / l_n \quad (13)$$

Among them, n_i the peak area obtained by integrating each fraction, l_i the lamellar thickness of each fraction calculated by using the Gibbs-Thomson equation, and f_i the relative content of each fraction.

Based on the above mathematical calculations, one can quantitatively analyze the results of thermal fractionation, and then explain its inherent physical meaning.

NEW DEVELOPMENT

According to the history of several general fractionation techniques mentioned above, early research targets focused on polyethylene copolymers. Because the disperse chain segment distribution of these hyperbranched polymers is excellent for this type of technique. In addition, these methods are also more common in researching the isotacticity and polymorphism, etc. of polypropylene. In the past two decades, with the rapid development of polymer science, the gene pool of polymer materials has been expanded exponentially, and the polyolefin family has grown stronger and stronger. These techniques are applicable far beyond the original polyethylene/propylene-based polymers, and we are finding them in more research on new materials, including other polyolefins [33–37], composites [38–43] and even some emerging polymers [44–70] or special block copolymers [71–76], for which, a series of polymer synthesis factors such as catalytic system and polymerization method, materials with different molecular chain structures will be formed. Polymer chemists used these fractionation methods to evaluate the quality of synthesis scheme, and polymer physicists paid more attention to the physical behavior caused by chain structure changes.

A bottleneck is gradually emerging for the development of the technique itself. Development of the technique comes not only from the continuous optimization of the parameters of the technique itself, but also from the combined use of more advanced characterization techniques. Müller et al. [26, 27] and other scholars [77] also made a series of adjustments to obtain the most optimum and universal experimental parameters for the fractionation of different systems.

We have also some thoughts on the modification of SSA fractionation technique for polyolefin elastomer recently [78]. We tried to add 5/10000 in weight linear polyethylene (LPE) into an ethylene-1-octene copolymer system by solution blending. For the original ethylene-1-octene copolymer, the introduction of about 40% (mass ratio) of octene copolymerization units severely branched the original ethylene–ethylene crystallizable sequence, resulting in a decrease in crystallinity and melting point. At the same time, the melting range is greatly broadened. Therefore, the melting point of an extremely small amount of LPE blended in is originally higher than the melting range

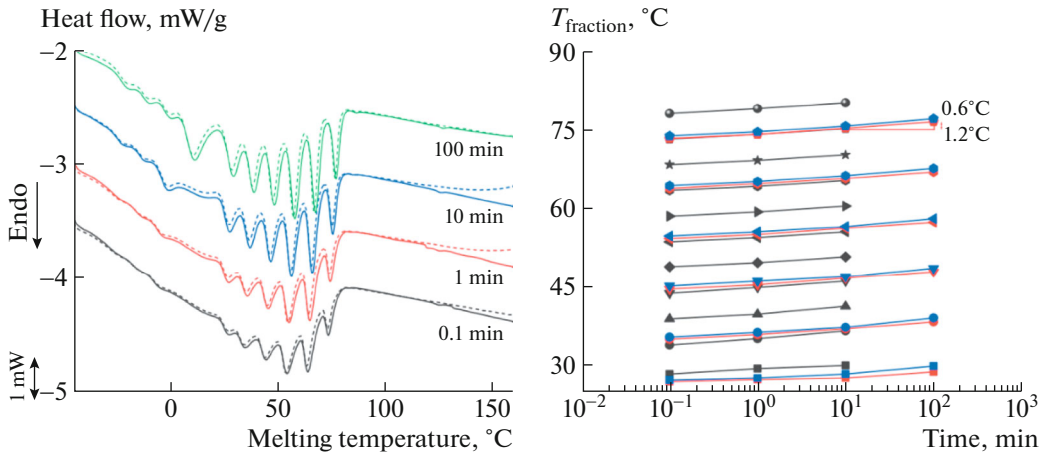

Fig. 13. Fractionation curves (Horizontal: degree Celsius, Vertical: heat flow) (left, solid: ethylene-co-octene, dashed: blends) and partial fraction's variation in melting point (right) of ethylene-1-octene copolymers and blends (black: 5°C intervals, blue: 10°C intervals (ethylene-*co*-octene), red: 10°C intervals (blends) (Horizontal: annealing time, Vertical: fraction temperature). Reprinted with permission of Springer from [78], Copyright 2022.

of the copolymer, which is equivalent to providing a crystal nucleus within the full melting range for the copolymer. The core part of SSA technique lies in the self-nucleation effect of each step, and when we provide a sufficiently strong crystal nucleus, will it affect its fractionation results?

The answer is yes. With the continuous extension of the annealing time of each step, the melting points of the fractions obtained by fractionation increase significantly, which also means that the crystallization is closer to completion, and the calculated branching parameters are also more accurate. The experimental results show that the presence of LPE nuclei throughout full-temperature regions can play the same role without affecting the effect of prolonged annealing time. From Fig. 13 right, one finds that the melting point is increased by about 1.2°C after the annealing time is extended by an order of magnitude, while the melting point is increased by about 0.6°C after the introduction of LPE nuclei.

The successful application of the modified SSA technique proposed above relies on an ideal mixing of the linear polymer with the random copolymer and the formation of enough stable crystalline nuclei whose amount is yet negligible in measurements. This is realized in polyethylene systems and still needs more polymer systems to verify.

PERSPECTIVE

In general, SSA thermal fractionation technique has been developed into a relatively standard scientific method. Therefore, it is difficult to achieve a more groundbreaking innovation. However, both SC and SSA fractionation are based on DSC measurements. With about 60 years of development in the same period as thermal fractionation technique, DSC has made revolutionary progress, including the emergence of fast scanning chip calorimetry (FSC).

The commercial FSC reaches already a heating rate of 2400 K/min and a cooling rate of 240 K/min. In addition, lab-developed FSC instruments possess a cooling rate up to tens of millions K/min giving us more imaginations. These figures far exceed the ramp rates of ~1–50 K/min that conventional DSC and High temperature stages can achieve. Thus, we may have the opportunity to apply FSC to the thermal fractionation experiments of some extreme systems. Indeed, Müller and colleagues have launched a preliminary attempt [79].

Besides, with the continuous development of in situ techniques, such as the application of the latest X-ray diffraction, Raman and infrared spectroscopy to characterize the thermal fractionation process of different systems in situ. These possibilities of in situ structural characterization during SSA experiments is sometimes very significant when the samples possess different competing polymorphous structures during crystallization such as in butene-1/ethylene random copolymer [80–82]. Such combinations of different techniques will help us not only better analyze the polymer structure information but also at the same time better understand and develop the inherent physical meaning of SSA fractionation means deeper. Finally, starting from the technique itself, the experimental design is improved through parameter control, and then the versatility of the SSA thermal fractionation technique is further improved.

FUNDING

This work is supported by the National Natural Science Foundation of China (U19B6001, 22161132007).

CONFLCIT OF INTEREST

The authors declare that they have no conflict of interest.

OPEN ACCESS

REFERENCES

1. H. Staudinger, *Macromolecular Chemistry: Nobel Lecture* (The Royal Swedish Academy of Sciences, Stockholm, 1953).
2. M. Y. Keating and E. F. McCord, Thermochim. Acta **243**, 129 (1994).
3. W. B. Hu, V. B. F. Mathot, R. G. Alamo, H. H. Gao, and X. J. Chen, Adv. Polym. Sci. **276**, 1 (2017).
4. B. Wunderlich, *Macromolecular Physics* (Acad. Press, New York, 1973).
5. V. Desreux, Recl. Trav. Chim. Pays-Bas **68**, 789 (1949).
6. V. Desreux and M. C. Spiegels, Bull. Soc. Chim. Belg. **59**, 476 (1950).
7. P. S. Francis, R. C. Cooke, and J. H. Elliott, J. Polym. Sci. **31** (123), 453 (1958).
8. S. L. Kita, K. Shirayama, I. Taniguchi, and T. Okada, in *Proceedings of Informal Meeting on Molecular Weight Distribution, Kyoto University, Japan, 1960* (Kyoto, 1960).
9. K. Shirayama, T. Okada, and S. L. Kita, J. Polym. Sci., Part A: Gen. Pap. **3**, 907 (1965).
10. C. Bergstrom and E. Avela, Kemia-Kemi **3**, 47 (1976).
11. C. Bergstrom and E. Avela, J. Appl. Polym. Sci. **23**, 163 (1979).
12. L. Wild, T. R. Ryle, D. C. Knobeloch, and I. R. Peat, J. Polym. Sci., Part B: Polym. Phys. **20**, 441 (1982).
13. T. Kamiya, N. Ishikawa, S. Kambe, I. Ikegami, H. Nishibu, and T. Hattori, ANTEC Proc. **48**, 871 (1990).
14. G. Balbontin, I. Camurati, T. Dallocco, A. Finotti, R. Franzese, and G. Vecellio, Angew. Makromol. Chem. **219**, 139 (1994).
15. M. J. Richardson, P. J. Flory, and J. B. Jackson, Polymer **4**, 221(1963).
16. J. Varga, J. Menczel, and A. Solti, J. Therm. Anal. **10**, 433 (1976).
17. J. Varga, J. Menczel, and A. Solti, J. Therm. Anal. **17**, 333 (1979).
18. J. Varga and F. Toth, Makromol. Chem., Macromol. Symp. **5**, 213 (1986).
19. H. W. Holden, J. Polym. Sci., Part C: Polym. Symp. **C 6**, 53 (1964).
20. A. P. Gray and K. Casey, J. Polym. Sci., Part B: Polym. Lett. **2**, 381 (1964).
21. B. Fillon, J. C. Wittmann, B. Lotz, and A. Thierry, J. Polym. Sci., Part B: Polym. Phys. **31**, 1383 (1993).
22. B. Fillon, B. Lotz, A. Thierry, and J. C. Wittmann, J. Polym. Sci., Part B: Polym. Phys. **31**, 1395 (1993).
23. B. Fillon, A. Thierry, J. C. Wittmann, and B. Lotz, J. Polym. Sci., Part B: Polym. Phys. **31**, 1407 (1993).
24. D. J. Blundell, A. Keller, and A. J. Kovacs, J. Polym. Sci., Part B: Polym. Lett. **4**, 481 (1966).
25. A. J. Müller, Z. H. Hernandez, M. L. Arnal, and J. J. Sanchez, Polym. Bull. **39**, 465 (1997).
26. A. J. Müller and M. L. Arnal, Prog. Polym. Sci. **30**, 559 (2005).
27. A. J. Müller, R. M. Michell, R. A. Perez, and A. T. Lorenzo, Eur. Polym. J. **65**, 132 (2015).
28. A. M. Thayer, Chem. Eng. News **73** (9), 15 (1995).
29. E. Adisson, M. Ribeiro, A. Deffieux, and M. Fontanille, Polymer **33**, 4337 (1992).
30. M. Q. Mang and S. E. Wanke, Polym. Eng. Sci. **43**, 1878 (2003).
31. M. Keating, I. H. Lee, and C. S. Wong, Thermochim. Acta **284**, 47 (1996).
32. F. Chen, R. A. Shanks, and G. Amarasinghe, Polym. Int. **53**, 1795 (2004).
33. A. T. Lorenzo, M. L. Arnal, A. J. Müller, A. B. de Fierro, and V. Abetz, Macromol. Chem. Phys. **207**, 39 (2006).
34. A. T. Lorenzo, M. L. Arnal, A. J. Müller, M. C. Lin, and H. L. Chen, Macromol. Chem. Phys. **212**, 2009 (2011).
35. T. Zheng, Q. Zhou, Q. Li, H. Y. Li, L. Y. Zhang, and Y. L. Hu, RSC Adv. **5**, 9328 (2015).
36. Y. P. Ma, W. P. Zheng, C. G. Liu, H. F. Shao, H. R. Nie, and A. H. He, Chin. J. Polym. Sci. **38**, 164 (2020).
37. T. Wen, H. J. Sun, B. Lotz, and S. Z. D. Cheng, Macromolecules **53**, 7570 (2020).
38. M. Trujillo, M. L. Arnal, A. J. Müller, S. Bredeau, D. Bonduel, P. Dubois, I. W. Hamley, and V. Castelletto, Macromolecules **41**, 2087 (2008).
39. F. A. He and L. M. Zhang, Polym. Test. **35**, 80 (2014).
40. J. Kang, J. H. He, Z. F. Chen, H. Y. Yu, J. Y. Chen, F. Yang, Y. Cao, and M. Xiang, J. Therm. Anal. Calorim. **119**, 1769 (2015).
41. J. K. Palacios, A. Sangroniz, J. I. Eguiazabal, A. Etxeberria, and A. J. Müller, Eur. Polym. J. **85**, 532 (2016).
42. Z. H. Hao, L. Li, B. Yang, X. Y. Sheng, X. Liao, L. L. He, and P. Liu, Polymers **11**, 433 (2019).
43. C. Habel, J. Maiz, J. L. Olmedo-Martinez, J. V. Lopez, J. Breu, and A. J. Müller, Polymer **202**, 12734 (2020).
44. M. A. Sabino, Polym. Degrad. Stab. **92**, 986 (2007).
45. R. M. Michell, A. J. Müller, G. Deshayes, and P. Dubois, Eur. Polym. J. **46**, 1334 (2010).
46. J. Luo, F. Huo, H. Lin, Z. L. Lin, Z. J. Chen, F. Yuan, H. L. Jiang, H. J. Wang, K. H. Tu, D. R. Liu, S. W. Tan,

and L. Q. Wang, J. Polym. Sci., Part B: Polym. Phys. **50**, 1277 (2012).

47. C. R. Snyder, R. C. Nieuwendaal, D. M. DeLongchamp, C. K. Luscombe, P. Sista, and S. D. Boyd, Macromolecules **47**, 3942 (2014).

48. R. A. Perez, M. E. Cordova, J. V. Lopez, J. N. Hoskins, B. Zhang, S. M. Grayson, and A. J. Müller, React. Funct. Polym. **80**, 71 (2014).

49. R. A. Perez, G. Saenz, S. Laurichesse, M. T. Casas, J. Puiggali, L. Averous, and A. J. Müller, J. Polym. Sci., Part B: Polym. Phys. **53**, 1736 (2015).

50. I. Arandia, A. Mugica, M. Zubitur, A. Arbe, G. Liu, D. Wang, R. Mincheva, P. Dubois, and A. J. Müller, Macromolecules **48**, 43 (2015).

51. I. Arandia, A. Mugica, M. Zubitur, A. Iturrospe, A. Arbe, G. M. Liu, D. J. Wang, R. Mincheva, P. Dubois, and A. J. Müller, J. Polym. Sci., Part B: Polym. Phys. **54**, 2346 (2016).

52. M. C. Righetti and M. L. Lorenzo, J. Therm. Anal. Calorim. **126**, 521 (2016).

53. J. V. Lopez, R. A. Perez, B. Y. Zhang, S. M. Grayson, and A. J. Müller, RSC. Adv. **6**, 48049 (2016).

54. T. P. Gumede, A. S. Luyt, M. K. Hassan, R. A. Perez-Camargo, A. Tercjak, and A. J. Müller, Polymers **9**, 709 (2017).

55. A. Kovalcik, R. A. Perez, C. Furst, P. Kucharczyk, and A. J. Müller, Polym. Degrad. Stab. **142**, 244 (2017).

56. D. Thomas and P. Cebe, J. Therm. Anal. Calorim. **127**, 885 (2017).

57. L. Sangroniz, R. G. Alamo, D. Cavallo, A. Santamaria, A. J. Müller, and A. Alegria, Macromolecules **51**, 3663 (2018).

58. T. P. Gumede, A. S. Luyt, and A. J. Müller, eXPRESS Polym. Lett. **12**, 505 (2018).

59. N. Zaldua, R. Lienard, T. Josse, M. Zubitur, A. Mugica, A. Iturrospe, A. Arbe, J. De Winter, O. Coulembier, and A. J. Müller, Macromolecules **51**, 1718 (2018).

60. M. C. Righetti, P. Marchese, M. Vannini, A. Celli, F. Tricoli, and C. Lorenzetti, Thermochim. Acta **677**, 186 (2019).

61. N. Zaldua, J. Maiz, A. de la Calle, S. Garcia-Arrieta, C. Elizetxea, I. Harismendy, A. Tercjak, and A. J. Müller, Polymers **11**, 1680 (2019).

62. X. N. Wen, Y. L. Su, Y. D. Shui, W. W. Zhao, A. J. Müller, and D. J. Wang, Macromolecules **52**, 1505 (2019).

63. R. A. Perez, R. d'Arcy, A. Iturrospe, A. Arbe, N. Tirelli, and A. J. Müller, Macromolecules **52**, 2093 (2019).

64. R. A. Perez, G. M. Liu, D. Cavallo, D. J. Wang, and A. J. Müller, Biomacromolecules **21**, 3420 (2020).

65. I. Arandia, L. Meabe, N. Aranburu, H. Sardon, D. Mecerreyes, and A. J. Müller, Macromolecules **53**, 669 (2020).

66. R. A. Perez, G. M. Liu, L. Meabe, Y. Zhao, H. Sardon, A. J. Müller, and D. J. Wang, Macromolecules **54**, 9670 (2021).

67. X. Liu and W. Yu, Macromolecules **54**, 3347 (2021).

68. X. Li, L. L. Wang, D. J. Wang, A. J. Müller, and X. Dong, Macromolecules **54**, 7552 (2021).

69. J. K. Palacios, A. Ben Fekih, C. Y. Argon, S. Irusta, S. Jestin, and S. Dagreou, Polym. Int. **70**, 1329 (2021).

70. C. B. Zhang, R. A. Perez, L. C. Zheng, Y. Zhao, G. M. Liu, L. Wang, and D. J. Wang, Polymer **222**, 123675 (2022).

71. Y. I. Denisova, G. A. Shandryuk, L. B. Krentsel, I. V. Blagodatskikh, A. S. Peregudov, A. D. Litmanovich, and Y. V. Kudryavtsev, Polym. Sci., Ser. A **55**, 385 (2013).

72. J. S. Fan, Q. L. Zhang, and J. C. Feng, Phys. Chem. Chem. Phys. **17**, 16158 (2015).

73. S. Holzer, T. N. Buttner, R. Schulze, M. M. L. Arras, F. H. Schacher, K. D. Jandt, and U. S. Schubert, Eur. Polym. J. **68**, 10 (2015).

74. G. A. Shandryuk, Y. I. Denisova, M. L. GringoIts, L. B. Krentsel, A. D. Litmanovich, E. S. Finkelshtein, and Y. V. Kudryavtsev, Eur. Polym. J. **86**, 143 (2017).

75. J. K.Palacios, G. M. Liu, D. J. Wang, N. Hadjichristidis, and A. J. Müller, Macromol. Chem. Phys. **220**, 1900292 (2019).

76. Y. I. Denisova, G. A. Shandryuk, M. P. Arinina, I. S. Levin, V. A. Zhigarev, M. L. Gringolts, E. S. Finkelshtein, A. Y. Malkin, and Y. V. Kudryavtsev, Polymers **13**, 1756 (2021).

77. Y. H. Xue, S. Q. Bo, and X. L. Ji, Acta Polym. Sin. **3**, 326 (2015).

78. X. T. Zhao and Y. F. Men, Chin. J. Polym. Sci. (2022). https://doi.org/10.1007/s10118-022-2740-2

79. D. Cavallo, A. T. Lorenzo, and A. J. Müller, J. Polym. Sci., Part B: Polym. Phys. **54**, 2200 (2016).

80. Y. T. Wang, Y. Lu, J. Y. Zhao, Z. Y. Jiang, and Y. F. Men, Macromolecules **47**, 8653 (2014).

81. Y. T. Wang, P. R. Liu, Y. Lu, and Y. F. Men, Chin. J. Polym. Sci. **34**, 1014 (2016).

82. Y. Q. Lai and Y. F. Men, Euro. Polym. J. **101**, 218 (2018).